

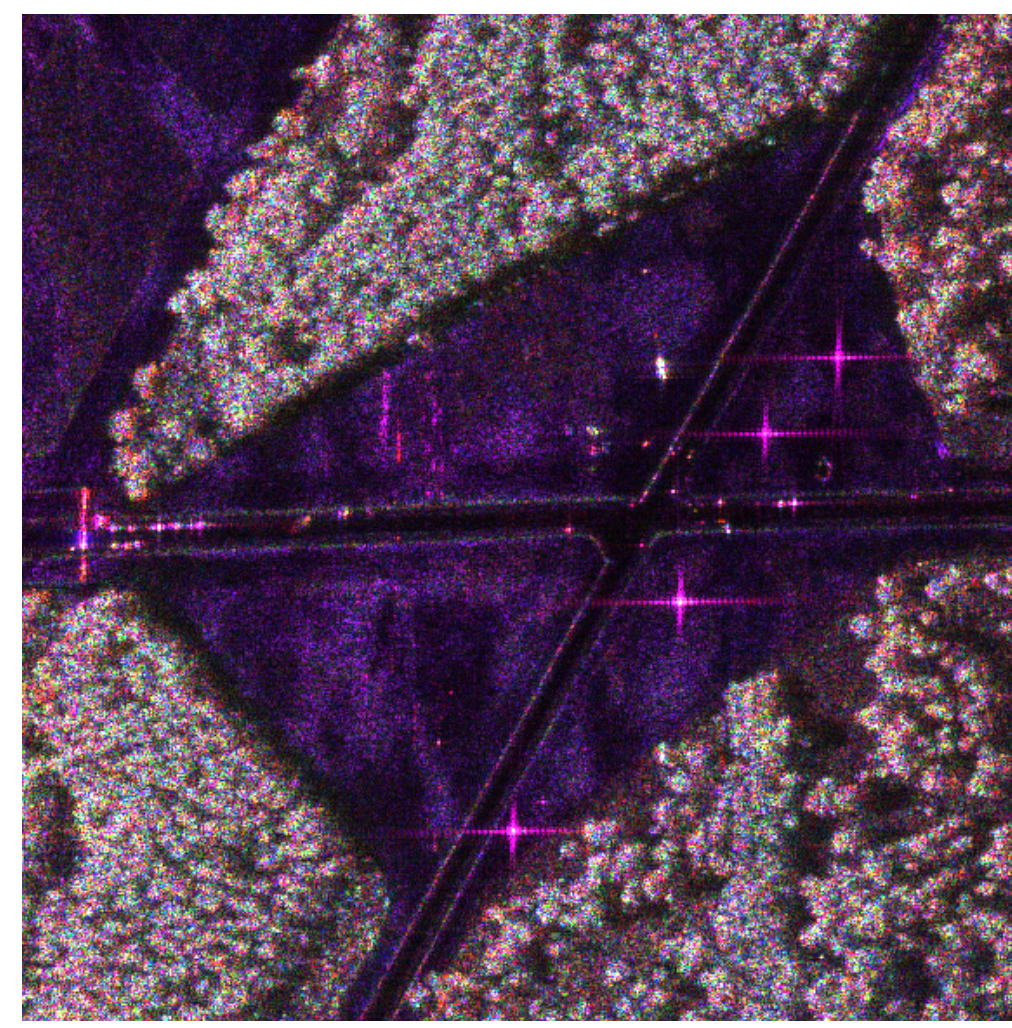
Anomaly detection

Anomalies refer to observations that deviate significantly from the **expected data pattern**. Anomaly detection in SAR imaging is challenging, due to the presence of *speckle* which induces many false positives and to the lack of *labeled data*.

Mathematical formulation:

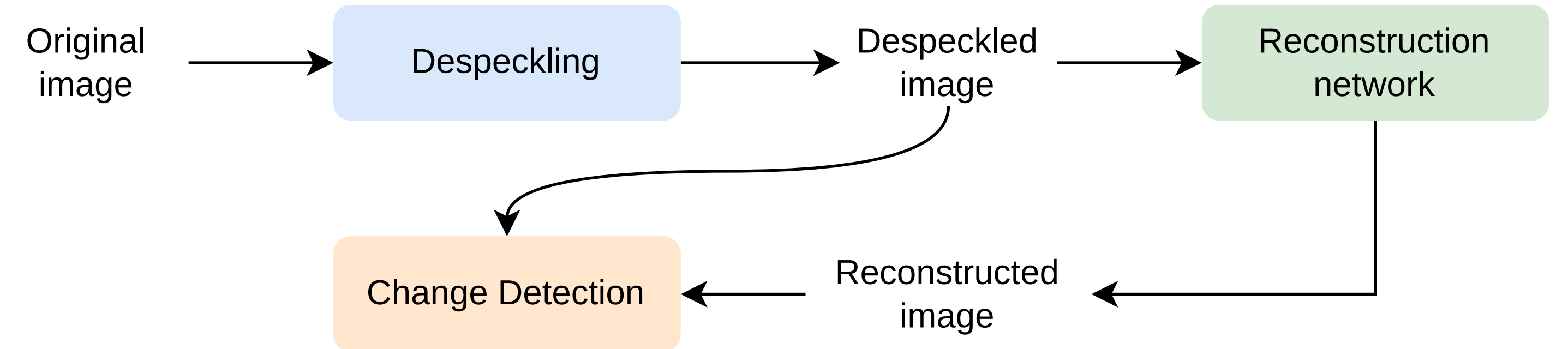
$$\begin{cases} H_0 : \theta_1 = \theta_2 \text{ (no anomaly),} \\ H_1 : \theta_1 \neq \theta_2 \text{ (anomaly),} \end{cases}$$

with θ_1 and θ_2 are estimated parameters vectors of the pixel values distribution.



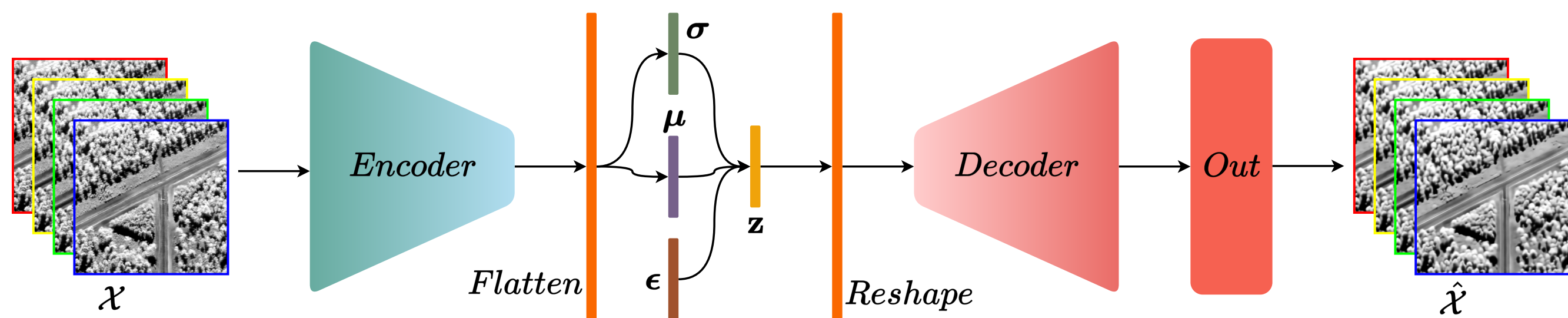
ONERA SETHI L-band image with anomalies.

Anomaly detection scheme



We adopt the anomaly detection methodology proposed in [3], which locates abnormal pixels by computing the deviation of a zone characteristics to the normal distribution. Instead of using the proposed AAE, we study an extension of the VAE family, called β -annealing VAE [2].

β -annealing VAE



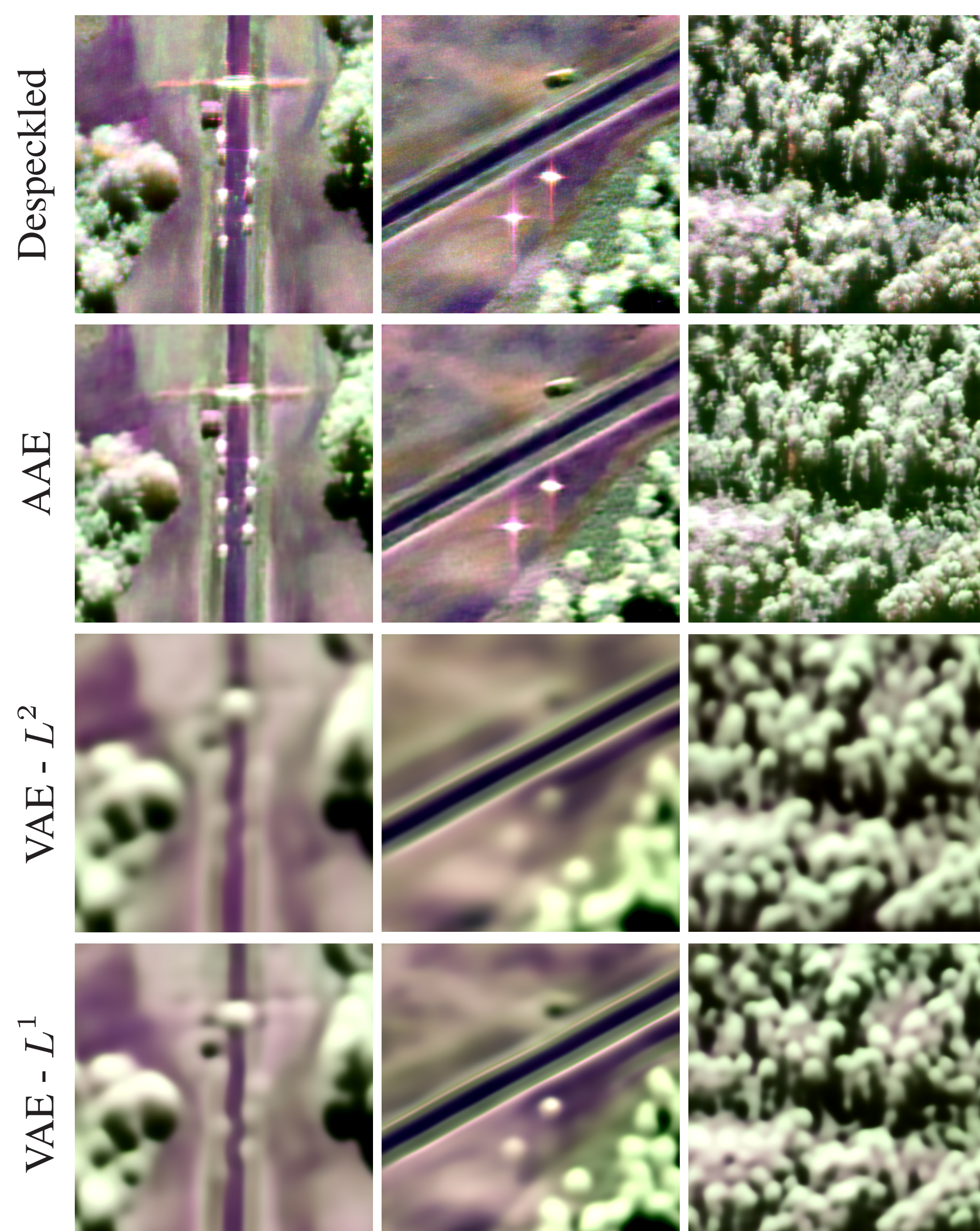
VAE architecture. \mathcal{X} and $\hat{\mathcal{X}}$ denote respectively despeckled and reconstructed SAR images. To obtain \mathcal{X} , we apply MERLIN algorithm [1] on a Side Look Complex SAR image.

Loss function:

Optimizing β -annealing VAE means minimizing the *Evidence Lower BOund* loss function, whose formulation is expressed as $\mathcal{L}_{ELBO} = \mathcal{L}_{rec} + \beta D_{KL}$ where \mathcal{L}_{rec} can be an L^1 or L^2 distance and

$$-D_{KL}(q(\mathbf{z}|\mathcal{X})||p(\mathbf{z})) = \frac{1}{2} \sum_{j=1}^J (1 + \log(\sigma_j^2) - \mu_j^2 - \sigma_j^2)$$

Reconstruction images:



Quantitative comparison:

Metrics	AAE	VAE - L^2	VAE - L^1
PSNR	33.19	31.46	32.41
SSIM[4]	0.866	0.886	0.892

Observations

Image reconstruction quality:

- Our VAE generates blurrier results than AAE's, but mitigates stronger high energetic targets.
- VAE with L^1 reconstruction loss outputs less blurry images than L^2

Anomaly map:

- Both AAE and VAE give lower false positives than Reed-Xiaoli detector.
- Reed-Xiaoli detector isolates better high-bounce targets.

Change detection

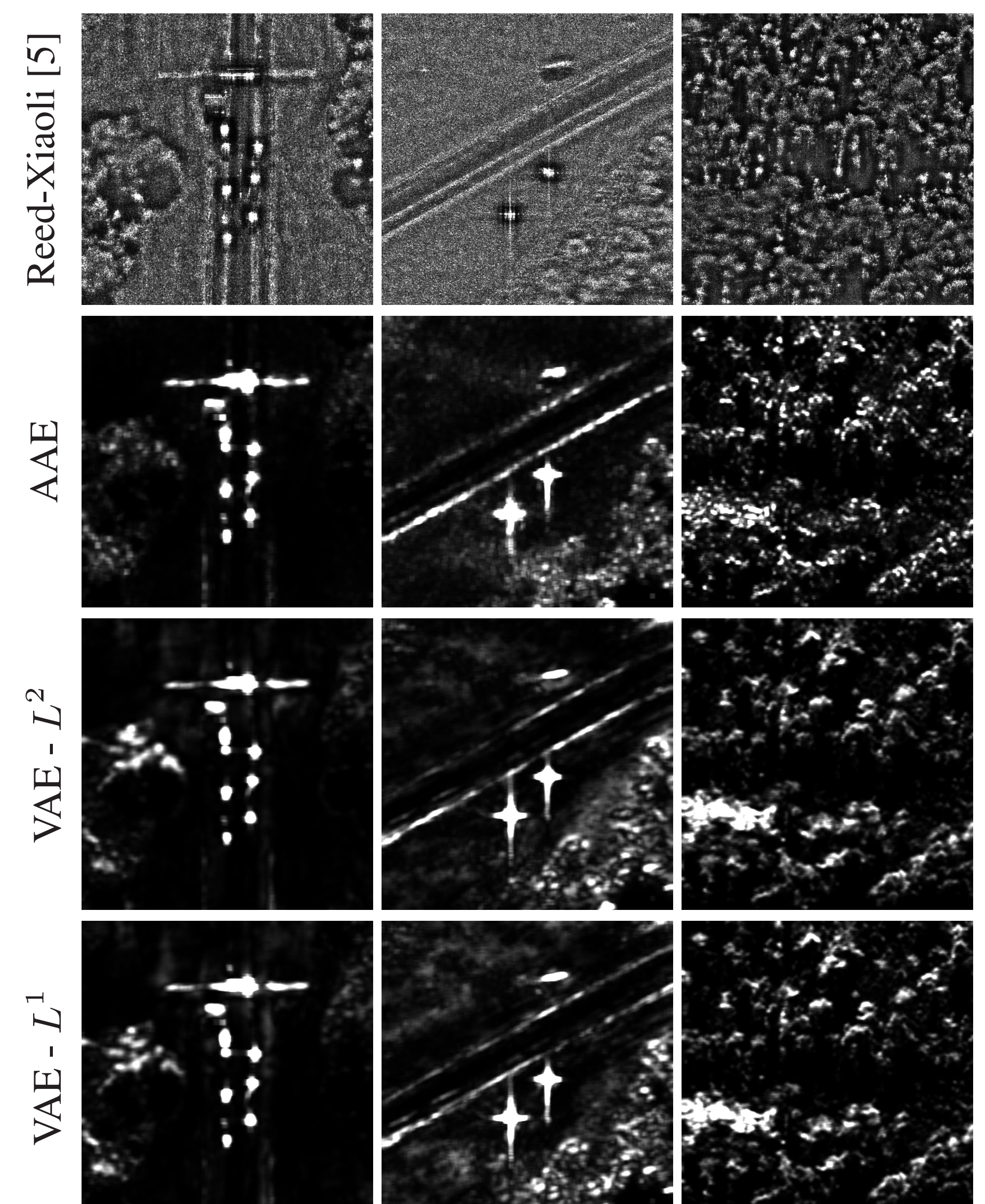
The anomaly detection process ends with the comparison between reconstructed images by the β -annealing VAE and the despeckled images. SAR images, having a high spatial and spectral dynamic range, therefore necessitate calculating statistics locally. We use the Frobenius norm as distance metric:

$$A_{k,l} = \left\| \hat{\Sigma}_{k,l}^{\hat{\mathcal{X}}} - \hat{\Sigma}_{k,l}^{\mathcal{X}} \right\|_F^2,$$

where $\Sigma_{k,l}$ denotes the Sample Covariance Matrix of *boxcar* $\mathcal{B}_{k,l}$, computed with the Sample Mean Vector $\hat{\mu}_{k,l}$:

$$\hat{\Sigma}_{k,l}^{\mathcal{X}} = \frac{1}{|\mathcal{B}_{k,l}|} \sum_{i,j \in \mathcal{B}_{k,l}} (\mathcal{X}_{i,j} - \hat{\mu}_{k,l}^{\mathcal{X}}) (\mathcal{X}_{i,j} - \hat{\mu}_{k,l}^{\mathcal{X}})^T,$$

Anomaly map:



References

- [1] E. Dalsasso, L. Denis, and F. Tupin. As if by magic: self-supervised training of deep despeckling networks with MERLIN. *IEEE Transactions on Geoscience and Remote Sensing*, 60:1–13, 2021.
- [2] H. Fu, C. Li, X. Liu, J. Gao, A. Celikyilmaz, and L. Carin. Cyclical annealing schedule: A simple approach to mitigating kl vanishing. *arXiv preprint arXiv:1903.10145*, 2019.
- [3] M. Muzeau, C. Ren, S. Angelliaume, M. Datcu, and J.-P. Ovarlez. Self-supervised learning based anomaly detection in synthetic aperture radar imaging. *IEEE Open Journal of Signal Processing*, 3:440–449, 2022.
- [4] Z. Wang, A. C. Bovik, H. R. Sheikh, and E. P. Simoncelli. Image quality assessment: from error visibility to structural similarity. *IEEE transactions on image processing*, 13(4):600–612, 2004.
- [5] X. Y. and I. S. Reed. Adaptive detection of signals with linear feature mappings and representations. *IEEE Transactions on Signal Processing*, 43(12):2953–2963, 1995.